



CHORUS

This is the accepted manuscript made available via CHORUS. The article has been published as:

Morphology of Lamellae-Forming Block Copolymer Films between Two Orthogonal Chemically Nanopatterned Striped Surfaces

Guoliang Liu, Abelardo Ramírez-Hernández, Hiroshi Yoshida, Kim Nygård, Dillip K.

Satopathy, Oliver Bunk, Juan J. de Pablo, and Paul F. Nealey

Phys. Rev. Lett. **108**, 065502 — Published 8 February 2012

DOI: [10.1103/PhysRevLett.108.065502](https://doi.org/10.1103/PhysRevLett.108.065502)

Morphology of Lamellae-forming Block Copolymer Films between Two Orthogonal Chemically Nanopatterned Striped Surfaces

Guoliang Liu^{1‡}, Abelardo Ramírez-Hernández^{1‡}, Hiroshi Yoshida², Kim Nygård³,
Dillip K. Satapathy³, Oliver Bunk³, Juan J. de Pablo^{1,*} and Paul F. Nealey^{1†}

¹*Department of Chemical and Biological Engineering,
University of Wisconsin-Madison, Madison, Wisconsin 53706, USA.*

²*Hitachi Ltd, Material Research Laboratory, Hitachi, Ibaraki 3191292, Japan.*

³*Department of Synchrotron Radiation and Nanotechnology,
Paul Scherrer Institut, CH-5232 Villigen, Switzerland*

(Dated: December 23, 2011)

The structure of block copolymers results from the interplay between weak intermolecular forces, typically in the order of $k_B T$ per molecule. This is particularly true for block copolymer thin films in the presence of chemically patterned surfaces, where the different contributions to the total free energy, the interfacial and bulk-like terms, have comparable magnitudes. Here, we report on the structures formed by block copolymer films equilibrated between two chemically patterned surfaces with orthogonal stripes. Our experiments and simulations reveal that the domains are continuous through the film and the interface between domains resembles the Scherk's first minimal surface. The impact of chemical patterns on block copolymer morphologies and the underlying physics gives insight into the nanofabrication of complex nanostructures with directed self-assembly using two engineered boundary conditions, as opposed to only one.

PACS numbers: 81.07.-b, 81.16.Dn, 83.80.Uv, 61.30.Hn

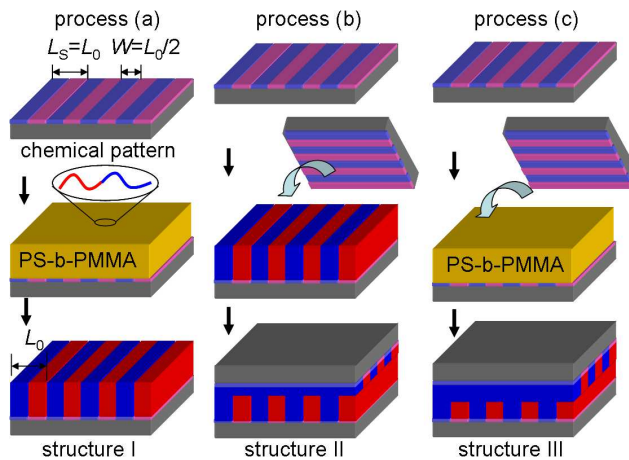


FIG. 1. Schematics of the directed self-assembly of block copolymers between two chemical patterns. In process (a), block copolymer is applied on the first chemical pattern, annealed to structure I. In process (b) after annealing on one chemical pattern, the block copolymer film is covered with the second chemical pattern, and re-annealed to structure II. In process (c), the block copolymer is applied on the first chemical pattern, covered with the second chemical pattern, and annealed to structure III.

Block copolymer molecules are chains composed of two or more chemically different polymers covalently bonded together. These materials have the inherent capability of self-assembling into structures whose dimensions range from 5 to 100 nm [1–3]. The dimensions and symmetry of the structures depend on the number of blocks, composition and architecture of the block copolymer. The assembly is thermodynamically governed by an interplay between two competing weak forces: *i*) the incompatibility between the blocks, which favors large domains and minimizes contacts between dissimilar blocks, and *ii*) the entropic force associated with the chain elasticity. The bulk morphologies arise as a compromise between these two factors. However, it is also because of the relative weakness of these forces that long-range order is typically not obtained in the bulk and defects form. In recent years, the directed assembly of block copolymer thin films has attracted abiding interest for fabrication of dense arrays of nanostructures [4]. Chemically patterned surfaces can control the orientation, dimensions and shapes of block copolymer domains. The equilibrium morphologies in thin films arise from a subtle interplay between the breaking of translational symmetry (due to one-dimensional confinement), energetic contributions of the patterns (attempting to induce, locally, a specific symmetry), structural frustration due to the incompatibility between the natural periodicity of the bulk morphology and film thickness, and the two weak forces mentioned above.

Directed assembly at the molecular level, as a bottom-up approach, has the advantages of sub-nanometer precision and a high degree of feature complexity [5, 6]. Furthermore, directed self-assembly of block copolymers on chemically patterned surfaces can generate 2D periodic structures such as arrays of lines and hexagonal close-packed spots [7, 8], and non-periodic device-oriented features [9–12]. As a result of thermodynamically driven self-assembly, these structures offer advanced properties such as high degrees of perfection, registration, feature dimension control [13, 14], size uniformity [15–19], and enhanced resolution [4, 10, 20–22]. Recent work demonstrates that chemical patterns can direct the block copolymers to self-assemble into a variety of 3D structures [23–25]. Much of the previous work focused on the directed self-assembly of block copolymers on one chemically patterned surface, and it would be of technological and scientific interest to further our fundamental understanding of the morphologies and physics of block copolymer self-assembly between two chemically patterned surfaces. Here we investigate the morphology of thin films of lamellae-forming block copolymers between two chemically nanopatterned surfaces that contain orthogonally-arranged preferentially-wetting stripes. We analyze the impact of chemical patterns on the formation and reconstruction of morphologies using scanning electron microscopy (SEM), small angle X-ray scattering (SAXS), and Monte Carlo simulations. The block copolymers form lamellae in registration with the corresponding chemical patterns near the bottom and top surfaces. To minimize the free energy, the nanodomains are bicontinuous and the interface separating domains resembles the Scherk’s first minimal surface, which is a surface composed of a doubly periodic array of saddle points.

The chemically patterned surfaces were prepared as described previously [10–12]. Using lithography and oxygen plasma, a PS brush on a silicon wafer was converted to chemical patterns with alternating stripes of PS brush and oxygen-plasma-treated PS brush, which preferentially wet PS and PMMA blocks of polystyrene-*block*-poly(methyl

methacrylate) (PS-*b*-PMMA), respectively. The period of the chemical patterns ($L_s = 76$ nm) was commensurate with that of PS-*b*-PMMA (molecular weight, $M_n = 85$ -91 kg mol⁻¹, bulk lamellae period, $L_0 = 75.8$ nm). All stripes had the same width ($W \approx 38$ nm). The largest chemically patterned surfaces used in this report span an area of 0.8 cm x 0.4 cm, but there is no upper limit to define chemical patterns with larger areas. The block copolymers were dissolved in toluene and spin-coated onto the chemically patterned substrate. By annealing at 230 °C for 3 days under vacuum, the block copolymers could self-assemble into periodic lamellae with domains in registration with the chemical patterns. To investigate the assembly of block copolymers between chemical patterns, we tested three processes which resulted in different structures, identified as structures I, II, and III, as shown in Fig. 1. All films had the same thickness of $2L_0$. The angle between the stripes on the bottom- and top-substrate was manually aligned to be about 90°. After assembly, the top-substrate was removed before characterization. Top-down SEM and SAXS in transmission mode were used to analyze the structures in real space and in reciprocal space, respectively.

Monte Carlo simulations were performed to offer 3D views of the structures and gain insight into the evolution of structure during directed assembly, which we could not visualize in real space through experiments. The model we use is a coarse-grained model for polymer melts whose origin is found in the standard Hamiltonian used in polymeric field theory [26, 27]. In our particle-based approach, the PS-PMMA block copolymers are represented by flexible linear chains described by the discretized Gaussian chain model, with $N = 16 + 16$ beads, with the position of the s^{th} bead in the i^{th} chain given by $\mathbf{r}_i(s)$. The non-bonded interactions take into account the repulsion between unlike monomers and the finite compressibility of the melt. This is expressed as the following functional: $\frac{\mathcal{H}_{\text{nb}}}{k_B T \sqrt{N}} = \int d\mathbf{r} [\chi N \phi_{\text{PS}} \phi_{\text{PMMA}} + \frac{\kappa N}{2} (\phi_{\text{PS}} + \phi_{\text{PMMA}} - 1)^2]$, where $\phi_\gamma(\mathbf{r})$ is the local dimensionless density of beads of type γ and $\bar{N} = (\rho_o R_e^3 / N)^2$, with ρ_o being the bead number density and R_e is the mean squared end-to-end distance of an ideal chain. To match the experimental conditions, we use $\kappa N = 85$, $\chi N = 63$ and $\sqrt{\bar{N}} = 167$. To model the thin films, the chains are confined by two impenetrable hard surfaces located in the planes $z = 0$ and $z = 2L_0$. The chemical pattern on each surface is represented by a one-body potential acting on each bead, that depends explicitly on the position and type of the bead, namely: $\frac{U(\mathbf{r}, \gamma)}{k_B T} = -\frac{\Lambda N f(x, y; \gamma)}{\xi / R_e} \exp\left[-\frac{z^2}{2\xi^2}\right]$ with $\Lambda N = 2$ and $f(x, y; \gamma)$ adopt values according the geometry of the pattern, and the position and type of the bead. The potential decays over a short distance $\xi = 0.15R_e$. The local densities are defined in a lattice with a spacing ΔL and computed from the beads positions by a particle-to-mesh interpolation [28, 29]. We sample configurations according to Metropolis criterion, $P_{\text{acc}} = \min[1, \exp(-\beta\Delta U)]$, where ΔU is the energy change between two configurations. More details of the simulations can be found elsewhere [30]. The agreement between model predictions and experiment has been established in the recent literature [24].

The top-down SEM images of structure I and II are shown in Fig. 2. After the assembly on one chemically patterned surface, the block copolymers formed lamellae in registration with the underlying chemical pattern [Fig. 2(a)], in agreement with previous reports. This pre-assembled film was then sandwiched with another chemically patterned surface. As can be seen in the top-down SEM image, the domains that ran originally in one direction are now organized in the orthogonal direction [Fig. 2(b)]. The block copolymer near the top surface re-assembled in response to the top chemical pattern during the second annealing step. Alignment marks were made on the sample to ensure that the images were taken in the same angle. The block copolymer domains at the top surface rotated an angle of approximately 87° to register with the top chemical pattern. The top-down view of structure III was similar to that of structure II (not shown). In this case, the film is not pre-assembled and the domains assemble from a disordered state.

Due to the probe depth of electrons, the top-down SEM gives real-space information of the block copolymer domains only near the free surface. SAXS, however, probes the entire film of block copolymer and gives volume-averaged reciprocal-space information to determine the morphology inside the film. The scattering measurement in transmission mode could detect the lamellar domains that were perpendicular to the substrate. For structure I, scattering peaks up to the fourth order were observed along the x -direction (the directions are defined in Fig. 3), and the odd-order peaks were more apparent than those even-order ones [Fig. 3(a)]. The scattering peaks indicated that the block copolymer formed perpendicular lamellae with a period of 76 nm in registration with the chemical pattern on the surface. For structure II, two sets of scattering peaks appeared on the x - y plane of the SAXS pattern, indicating the coexistence of the block copolymer lamellar domains perpendicular to the plane of the film along the two directions [Fig. 3(b)]. The angle between the x and y directions was $\approx 87^\circ$, as measured from the SAXS pattern, which was in agreement with the rotation angle measured from the SEM images. In comparison with the scattering pattern in Fig. 3(a), the appearance of the second set of scattering peaks in Fig. 3(b) was a result of the re-assembly during the second annealing step, indicating that the block copolymer domains near the top surface re-assembled to align with the chemical pattern on the top substrate. The scattering intensities of the peaks along the y -direction were not as strong as those along the x -direction, indicating that the volume fraction of the lamellae oriented along

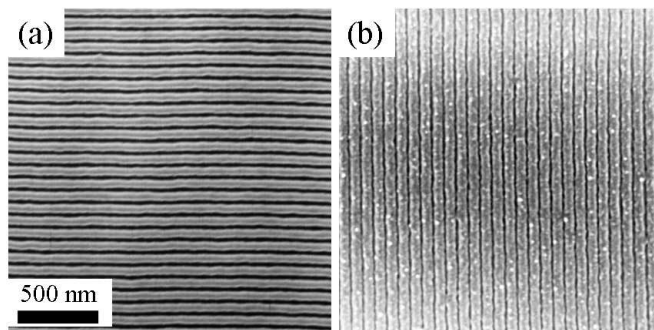


FIG. 2. Top-down SEM images of (a) structure I and (b) structure II. The lamellae domains in (b) rotate 87° with respect to those in (a) after the re-assembly, as measured in SEM. PS and PMMA domains appear bright and dark, respectively. The white spots in (b) are debris of silicon and silicon oxide after mechanically peeling-off the top-substrate. The scale bar applies to all SEM images.

the y -direction was smaller than that along the x -direction. Based on the intensity of the scattering peaks along the two directions, approximately 17% volume percent (assuming that the domains are either x or y aligned) of the film re-arranged to register with the chemical pattern parallel to the y -direction during the second annealing step. For structure III, two sets of scattering peaks with approximately the same intensities were observed along the x - and y -direction [Fig. 3(c)]. The roughly equal scattering intensities of the peaks along the two directions indicated that the lamellar domains near the top and the bottom substrate had roughly equal volume fraction and they met in the middle of the film. Estimated from the scattering measurement, for this particular sample, 63% of film had lamellae domains oriented in the y -direction.

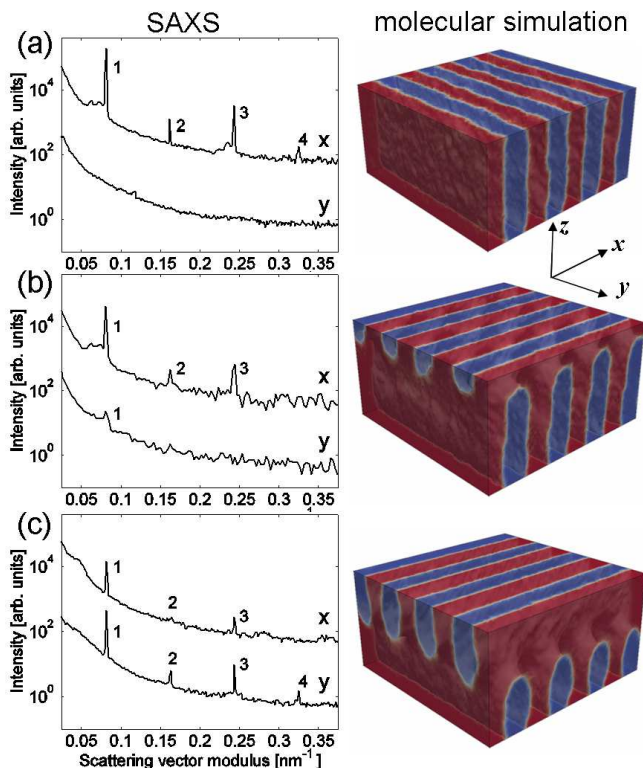


FIG. 3. Spectra of SAXS in transmission mode along the x and y directions, and the molecular simulated 3D views of (a) structure I, (b) structure II, and (c) structure III. The X-rays travel along the z -direction, enabling the scattering intensities to be collected on the x - y plane. The angle between x and y is 87° , as measured in 2D SAXS pattern. The intensities are offset for clarity. The numbers highlight the scattering peaks characteristic of lamellae morphology. Red and blue represent the PS-rich and PMMA-rich domains, respectively [35].

The 3D morphologies obtained from Monte Carlo simulations of structure I, II, and III revealed the formation of a single lamellae morphology on one chemical pattern and a complex structure between two chemical patterns. The complex structure consisted of lamellar domains, replicating the patterns, continuously connected by an interface characterized by an array of saddle points located in a plane, whose localization depends on the process, in agreement with SAXS measurements.

The formation and localization of the interface can be explained by the minimization of free energy in the system. By localization, we mean the position of the plane where the saddle points defining the interface are located. Starting with a disordered state on one chemical pattern, as expected, the block copolymer equilibrates at lamellae in registration with the underlying chemical pattern [Fig. 3(a)]. Starting with a disordered state followed by an intermediate state in which a lamellae is placed between two chemical patterns, the bottom part of the block copolymer film remains, but the top part re-assembles in response to the chemical pattern on the top substrate [Fig. 3(b)]. Once the annealed block copolymer lamellae are exposed to a chemical pattern on the top substrate, the increased block-surface interfacial energy initiates the directed self-assembly of the block copolymers near the top surface. The lamellar domains rearrange so that they are in registration with the corresponding wetting stripes to minimize the surface energy. The range of interactions between the chemical pattern and block copolymer is a few nanometers. The reorganization of more material according to the top pattern requires collective distortion of the bottom lamellae, thus once the influence of the pattern decays, the interface connecting the domains forms. The entropy penalty of the block copolymer chains being near the surface and the energetic requirement to satisfy the boundary conditions of the chemical patterns compete with the chain frustration induced by the non-flat regions of the interface. The balance of these competing elements induces the formation of the interface far from the surface. But as long as the interface is far enough from the surface, it can be localized anywhere inside the film. The lack of thermodynamic driving force results in the localization of the interface near the top surface. In Monte Carlo (MC) simulations, even after 10^5 MC steps, we do not observe any shift of the interface towards the middle of the film, indicating that the morphology is stable. When the block copolymer self-assembly is directed by two chemical patterns from a disordered state, the top and bottom patterns induce the formation of lamellae domains at approximately the same rate, thus the interface forms in the middle of the film [Fig. 3(c)]. Although the boundary conditions are the same at the end of both process (b) and (c), the resulting block copolymer structures are different due to the presence of an intermediate state in process (b). Nevertheless, both structures have the same free energy.

In general, the nucleation rate of each pattern could be different (for example, maybe the initial assembly occurs already in the spin coating process on one chemical pattern) and the interface can be localized anywhere inside the film as long as it is far enough from the surfaces [36]. This interface resembles the interface predicted at grain boundaries between two lamellar grains of different orientations in the bulk. In our case, however, the structure and the associated interface corresponded to a *bona fide* thermodynamic equilibrium. In the bulk, under the constraints of volume conservation for each component and the minimization of interfacial energy between PS and PMMA domains, the interface between the two orthogonal lamellar grains was predicted to be described by the Scherk's first minimal surface with a mean curvature of zero [31, 32]. This was similar to surfactant systems in bulk, in which Belushkin *et. al* [33] found with a Ginzburg-Landau model that the grain boundary between two orthogonal lamellar grains was a good approximation of a minimal surface and was well described by the Scherk's first surface. Thus, our simulations showed that the formation of the interface between domains resulted in a bicontinuous and double-periodic structure.

In this work, we demonstrate the directed self-assembly of block copolymers into 3D structures between two chemically nanopatterned substrates. Top-down SEM, transmission-mode SAXS, and molecular simulations offer insights into the formation and reorganization of structures in response to the chemical patterns. The directed self-assembly from both top and bottom surfaces offers precise surface property control for block copolymers that have a significant surface energy difference between the two blocks and it can avoid the formation of undesired structures at the surface for lithographic applications. The formation of a complex interface results in bicontinuous block copolymer domains through the entire film. This continuity implies important physical properties such as continuous conductivity, diffusivity, etc. which are desirable for technological applications. Examples are photovoltaic devices where excitons require continuous conduction to the electrodes during their short lifetime so that they do not diminish at the interfaces [34], and energy storage devices such as batteries where electricity carriers require continuous diffusivity towards the electrodes. We present in this letter a simple example of directed self-assembly of symmetric diblock copolymers between simple chemical patterns, but the methodology and underlying physics can be extended to sophisticated block polymers, complex chemical patterns and 3D architectures.

This work was supported by the Semiconductor Research Corporation and NSF through the UW-Nanoscale Science and Engineering Center (Grant No. DMR0832760).

* depablo@engr.wisc.edu

† nealey@engr.wisc.edu

- [1] F. S. Bates and G. H. Fredrickson, Annual Review of Physical Chemistry **41**, 525 (1999).
- [2] F. S. Bates, and G. H. Fredrickson, Physics Today **52**, 32 (1999).
- [3] I. W. Hamley, *The Physics of Block Copolymers* Oxford University Press, 1998.
- [4] R. Ruiz, et al., Science **321**, 936 (2008).
- [5] G. M. Whitesides and B. Grzybowski, Science **295**, 2418 (2002).
- [6] Y. D. Xia, et al., Polymer **49**, 5596 (2008).
- [7] C. Park, J. Yoon, and E. L. Thomas, Polymer **44**, 6725 (2003).
- [8] M. Park, et al. Science **276**, 1401 (1997).
- [9] G. M. Wilmes, et al., Macromolecules **39**, 2435 (2006).
- [10] G. Liu, et al., Adv. Funct. Mater. **20**, 1251 (2010).
- [11] M. P. Stoykovich, et al., ACS Nano **1**, 168 (2007).
- [12] M. P. Stoykovich, et al., Science **308**, 1442 (2005).
- [13] G. Liu, et al., Macromolecules **42**, 3063 (2009).
- [14] K. O. Stuen, et al., Macromolecules **42**, 5139 (2009).
- [15] M. P. Stoykovich and P. F. Nealey, Materials Today **9**, 20 (2006).
- [16] S. O. Kim, et al. Nature **424**, 411 (2003).
- [17] E. W. Edwards, et al., Macromolecules **40**, 90 (2007).
- [18] K. C. Daoulas, et al., Langmuir **24**, 1284 (2008).
- [19] M. P. Stoykovich, et al., Macromolecules **43**, 2334 (2010).
- [20] I. Bitai, et al., Science **321**, 939 (2008).
- [21] Y. Tada, et al., Polymer **50**, 4250 (2009).
- [22] J. Y. Cheng, et al., Adv. Mater. **20**, 3155 (2008).
- [23] K. C. Daoulas, et al. Phys. Rev. Lett. **96**, 036104 (2006).
- [24] F. A. Detcheverry, G. Liu, P. F. Nealey and J. J. de Pablo, Macromolecules **43**, 3446 (2010).
- [25] G. Liu, et al., Photopolym Sci. Technol. **23**, 149 (2010).
- [26] G. H. Fredrickson, *The Equilibrium Theory of Inhomogeneous Polymers* Oxford, 2006.
- [27] M. W. Matsen, J. Phys.: Condens. Matter, **14** R21 (2002).
- [28] F. A. Detcheverry, H. Kang, K. Ch. Daoulas, M. Müller, P. F. Nealey, and J. J. de Pablo, Macromolecules **41** 4989 (2008).
- [29] F. A. Detcheverry, D. Q. Pike, U. Nagpal, P. F. Nealey and J. J. de Pablo, Soft Matter **5**, 4858 (2009).
- [30] A. Ramírez-Hernández, G. Liu, P. F. Nealey and J. J. de Pablo, to be published.
- [31] E. L. Thomas, et al., Nature **334**, 598 (1988).
- [32] S. P. Gido, et al., Macromolecules **26**, 4506 (1993).
- [33] M. Belushkin and G. Gompper, J. Chem. Phys. **130**, 134712 (2009).
- [34] S. B. Darling, Energy Environ. Sci. **2** 1266 (2009)
- [35] Images were created using Paraview, an Open-Source Scientific Visualization Software, <http://www.paraview.org/>.
- [36] See Supplemental Material at [URL will be inserted by publisher] for details concerning the role of kinetics on the interface localization inside the film, and simulation results supporting the corresponding reasoning.